

From Low-Dimensional Synchronous Chaos to High-Dimensional Desynchronous Spatiotemporal Chaos in Coupled Systems

Gang Hu,^{1,2} Ying Zhang,³ Hilda A. Cerdeira,⁴ and Shigang Chen³

¹Chinese Center for Advanced Science and Technology (World Laboratory), Beijing 8730, China

²Department of Physics, Beijing Normal University, Beijing 100875, China

³LCP, Institute of Applied Physics and Computational Mathematics, P.O. Box 8009(26), Beijing 100088, China

⁴The Abdus Salam International Centre for Theoretical Physics, P.O. Box 586, 34100 Trieste, Italy

(Received 8 March 2000)

The dynamic behavior of coupled chaotic oscillators is investigated. For small coupling, chaotic state undergoes a transition from a spatially disordered phase to an ordered phase with an orientation symmetry breaking. For large coupling, a transition from full synchronization to partial synchronization with translation symmetry breaking is observed. Two bifurcation branches, one in-phase branch starting from synchronous chaos and the other antiphase branch bifurcated from spatially random chaos, are identified by varying coupling strength ϵ . Hysteresis, bistability, and first-order transitions between these two branches are observed.

PACS numbers: 05.45.Xt, 05.45.Jn

Recently, the study of variation from low-dimensional chaos to high-dimensional spatiotemporal chaos has attracted much attention. In this study, systems of coupled chaotic oscillators serve as very convenient models and have been investigated extensively [1]. By increasing coupling between the oscillators, the dimension of the system state may be changed from high-dimensional desynchronous chaos to low-dimensional synchronous chaos, and it is interesting to investigate the characteristic features in this variation.

By varying the coupling, the coupled systems usually undergo complicated bifurcations, manifest very rich pattern formation behavior, and exhibit a variety of synchronization behaviors, such as exact synchronization for coupled identical systems [1], clustering (partial synchronization) for globally coupled system [2], phase synchronization and lag synchronization for nonidentical chaotic oscillators [3], and so on.

Often, various pattern formations and synchronization-desynchronization transitions are associated with and even originated from different kinds of symmetry breaking, and thus a thorough investigation of the symmetry breaking behavior becomes very useful for understanding the mechanism underlying the complexity and the global spatiotemporal bifurcation scenarios of the system. This understanding is extremely important for the wide applications of the coupled oscillators, such as laser array and coupled Josephson junctions. In this Letter we will attack this problem by considering a model system extensively investigated—coupled Rossler oscillators.

The coupled system with a spatial, periodic, boundary condition is given as

$$\begin{aligned} \dot{x}_i &= -y_i - z_i + \epsilon(x_{i+1} + x_{i-1} - 2x_i), \\ \dot{y}_i &= x_i + ay_i + \epsilon(y_{i+1} + y_{i-1} - 2y_i), \\ \dot{z}_i &= b + (x_i - c)z_i + \epsilon(z_{i+1} + z_{i-1} - 2z_i), \\ x_{i+N} &= x_i, \quad y_{i+N} = y_i, \quad z_{i+N} = z_i. \end{aligned} \quad (1)$$

For $a = 0.45$, $b = 2.0$, and $c = 4.0$, the single Rossler oscillator is chaotic [see Fig. 1(a)]. In the following, we fix the system size to $N = 6$, which is large enough to show rich spatial patterns while sufficiently small for

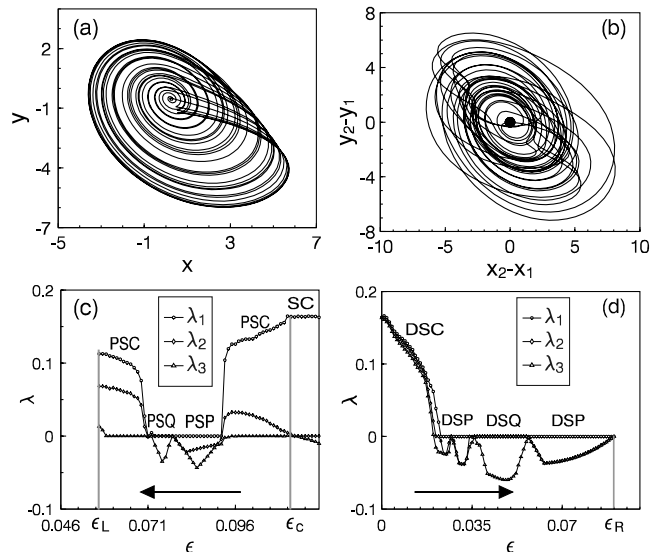


FIG. 1. Simulation of Eqs. (1), $a = 0.45$, $b = 2.0$, $c = 4.0$, and $N = 6$. These parameters will be used in all the following figures. (a) $\epsilon = 0$, the projection of a chaotic trajectory of a single Rossler oscillator in the x - y plane. (b) The projections of $\vec{r}_2(t) - \vec{r}_1(t)$ in the x - y plane, i.e., $y_2(t) - y_1(t)$ vs $x_2(t) - x_1(t)$. The black disk at the origin for $\epsilon > \epsilon_c = 0.111$, the other trajectory for $\epsilon = 0$. (c) The largest three Lyapunov exponents vs ϵ . We start from $\epsilon > \epsilon_c$. SC: synchronous chaos; PSC: partially synchronous chaos; PSP: partially synchronous periodic motion; PSQ: partially synchronous quasiperiodic motion. (d) The same as (c) but starting from $\epsilon = 0$. DSC: desynchronous chaos; DSP: desynchronous periodic state; DSQ: desynchronous quasiperiodic state. At $\epsilon_R = 0.090$ ($\epsilon_L = 0.056$) the branch (d) [(c)] jumps to the branch (c) [(d)] from the DSP state to the PSP state [from the PSC state to the DSQ state] via saddle-node bifurcation.

convenient numerical simulations. The extension to larger systems will be discussed in the conclusion. For sufficiently large coupling ($\epsilon > \epsilon_c = 0.111$ for $N = 6$) all oscillators perform low-dimensional synchronous chaotic motion [see the disk at $x = y = 0$ in Fig. 1(b)]. Without coupling $\epsilon = 0$, all oscillators also perform chaotic motions of the single oscillator; however, different oscillators have desynchronous trajectories [see Fig. 1(b)]. Thus, the whole six-cell system has a large dimension (6 times larger than the synchronized system). It is interesting to note that both the synchronous chaotic state (for $\epsilon > \epsilon_c$) and the completely desynchronous state (for $\epsilon = 0$) are spatially symmetric in the sense that any exchange $i \rightleftharpoons j$, $i, j = 1, 2, \dots, 6$, does not change the system state. Therefore, we call these two states completely symmetric states. Nevertheless, the symmetries of both states are essentially different; the synchronous chaos has symmetry at any instant, i.e., $\vec{r}_i(t) = \vec{r}_j(t)$ is valid for any sites and at any times, while the desynchronous chaos of $\epsilon = 0$ has symmetry for a long time average only, i.e., $\langle A_i \rangle = \langle A_j \rangle$ is valid for all sites with $\langle A_i \rangle = \langle A_j \rangle = \lim_{T \rightarrow \infty} \frac{1}{T} \int_0^T A(\vec{r}_i(t)) dt$. Therefore, we call the former “microscopic” symmetry resulted from dynamics at strong coupling while the latter “macroscopic” symmetry due to the uncoupling and identity of oscillators. It is interesting to investigate the rich patterns and bifurcations associated with the symmetry and synchronization variation, by varying ϵ between zero and $\epsilon > \epsilon_c$.

First, we study the Lyapunov spectrum of the system by varying the coupling strength ϵ in Figs. 1(c) and 1(d); the three largest Lyapunov exponents are plotted. The Lyapunov exponents are computed as follows. In (c) we decrease ϵ from $\epsilon > \epsilon_c$ in the step $\Delta\epsilon = 0.001$. For each ϵ we run the system [Eqs. (1)] by taking the ending state for the previous coupling as the initial state for the current coupling. Small noise is used for excluding unstable states. All the Lyapunov exponents vary continuously until $\epsilon = \epsilon_L \approx 0.056$, lower than which the system jumps to the state of Fig. 1(d). In 1(d) we do the same as 1(c) while by increasing ϵ from zero; this branch of state is ended at $\epsilon = \epsilon_R \approx 0.090$, over which the system jumps to the state of 1(c). Therefore, we have a large hysteresis loop, and the system is bistable between ϵ_L and ϵ_R .

In Fig. 1(c), the state SC for $\epsilon > \epsilon_c$ indicates synchronous chaos where all oscillators perform identical chaotic motion of Fig. 1(a). As ϵ decreases smaller than ϵ_c , synchronization of oscillators breaks via on-off intermittency, however, only partially. Then we find an interesting spatial structure *abcbad*, i.e., oscillators from 1–6 sites perform four distinctive chaotic trajectories $a(t)$, $b(t)$, $c(t)$, and $d(t)$ in the spatial order of 1, 5 sites— $a(t)$, 2, 4— $b(t)$, 3— $c(t)$, and 6— $d(t)$. Therefore, the state has two pairs of oscillators (1, 5) and (2, 4) which still keep their pair synchronization as the full synchronization breaks. The transition of synchronization breaking is associated with the breaking of translation symmetry of the system. We call this state the partially synchronous

chaotic state PSC. Partial synchronization of chaotic oscillators has been extensively investigated in globally coupled systems, where no space structure can be involved [2]. Recently, partial synchronization in asymmetrically coupled systems has been reported [4]. To our knowledge, it is the first time that a partial chaotic synchronization with typical spatial structure appears spontaneously in symmetrically and locally coupled systems. Further decreasing ϵ to $\epsilon < 0.092$, the *abcbad* PSC state turns to be a partially synchronous periodic state (PSP) with the same *abcbad* spatial structure. As $\epsilon < 0.078$, the *abcbad* PSP state is replaced by a partially synchronous quasiperiodic state (PSQ) via Hopf bifurcation with the same spatial *abcbad* structure. For $\epsilon < 0.070$, this PSQ bifurcates again to the PSC chaotic *abcbad* state. After $\epsilon < \epsilon_L$, the branch of stable solution [Fig. 1(c)] stops to exist; the system jumps to the state of Fig. 1(d).

In Fig. 1(d) we find, for small ϵ , all six oscillators take chaotic motions, desynchronized from each other, called the desynchronous chaotic state (DSC). Increasing ϵ to $\epsilon > 0.022$, the DSC state bifurcates to the desynchronous periodic state (DSP). Further increasing ϵ to $\epsilon > 0.034$, the DSP state is replaced by a desynchronous quasiperiodic (DSQ). For $\epsilon > 0.057$, this DSQ bifurcates again to a desynchronous periodic state DSP. After $\epsilon > \epsilon_R$, the Fig. 1(d) branch no longer exists and the system jumps to the branch of Fig. 1(c).

Previously, we presented some numerical observations of rich bifurcations and patterns by varying the coupling strength. In order to conduct a more quantitative analysis and to obtain a more comprehensive understanding, we use the lag function and the phase synchronization suggested in Ref. [3].

We define a lag function, based on the $x(t)$ variable in Eqs. (1), as

$$S_{ij}(\tau) = \sqrt{\frac{\langle [x_i(t) - x_j(t - \tau)]^2 \rangle}{\langle x_i^2(t) \rangle \langle x_j^2(t) \rangle^{1/2}}} \quad i, j = 1, 2, \dots, 6, \quad (2)$$

$$\langle f(x) \rangle = \lim_{T \rightarrow \infty} \frac{1}{T} \int_0^T f(x) dx.$$

If $x_i(t)$ and $x_j(t)$ take the same chaotic attractor while they have completely uncorrelated trajectories, we have $S_{ij}(\tau) \equiv \sqrt{2}$, while if they are identical with certain phase shift (denoted by τ_0 time shift) we have $S_{ij}(\tau_0) = 0$. Otherwise, the $S_{ij}(\tau)$ function may oscillate with τ around $\sqrt{2}$ without reaching zero.

Figure 2 shows the lag functions for various ϵ by taking an average time $T = 6 \times 10^5$, which is sufficiently long for eliminating the transient. In Figs. 2(a)–2(c), we show mutual lag functions $[S_{ij}(\tau), j = i + 3]$ for various ϵ in the Fig. 1(d) branch. For $\epsilon = 0.005$ we found $S_{ij}(\tau) \approx \sqrt{2}$ for any τ , implying that the crossing correlation is negligible after long time average. For $\epsilon = 0.014$, a finite deviation of $S_{ij}(\tau)$ from $\sqrt{2}$ is clearly manifested; it definitely shows certain collective motion between different sites. For $\epsilon = 0.085$, which is in a DSP region,

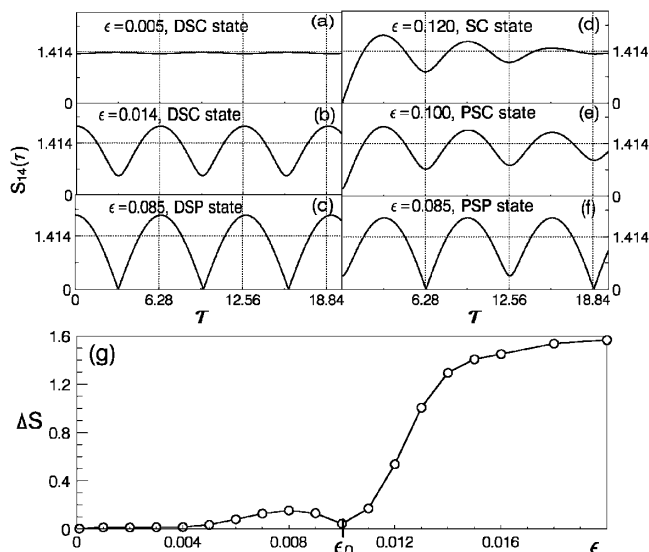


FIG. 2. Lag functions $S_{14}(\tau)$ defined in Eq. (2) for different ϵ . (a), (b), (c) For the state in the Fig. 1(d) branch. (d), (e), (f) For the Fig. 1(c) branch. (g) The order parameter ΔS , defined in Eq. (3), plotted vs ϵ in the Fig. 1(d) branch. For $\epsilon < \epsilon_0$ the system is in a disordered state. The order parameter increases rapidly after $\epsilon > \epsilon_0$.

we found that $S_{ij}(\tau)$ is periodic and $S_{ii+3}(\tau) = 0$ for $\tau = \frac{(2n+1)T_0}{2}$ with T_0 being the period, indicating that the motion of the $(i+3)$ th oscillator is identical to the motion of the i th oscillator with a time shift of $\frac{T_0}{2}$. In Figs. 2(d)–2(f), we show $S_{ii+3}(\tau)$ for various ϵ in the Fig. 1(c) branch. It is shown that $S_{ij}(\tau)$ has a large deviation from $\sqrt{2}$ in all the SC, PSC, and PSP regions, indicating that strong coherence exists in this entire branch.

From Fig. 2(a) some significant characteristics should be emphasized. For $\epsilon = 0.005$, we have $S_{ij}(\tau) \approx \sqrt{2}$, corresponding to a dead spatially disordered state. Deviation of $S_{ij}(\tau)$ from $\sqrt{2}$ for $\epsilon = 0.014$ represents the life of mutual correlation. An interesting point is that both parameters $\epsilon = 0.005$ and $\epsilon = 0.014$ belong to the region of DSC; the essentially different features of $S_{ij}(\tau)$ indicate that a new bifurcation not revealed by the Lyapunov analysis in Fig. 1(d) should exist in this DSC region. In order to quantitatively measure the spatial ordering, we define the following quantity as an order parameter:

$$\Delta S = \sqrt{2} - \min[S_{ii+3}(\tau)]. \quad (3)$$

Very small ΔS shows disorder between the oscillators, while large ΔS indicates strong spatial coherence. In Fig. 2(g), we plot ΔS vs ϵ by increasing ϵ from zero [the branch of Fig. 1(d)], and find this order parameter is very small for small ϵ ($\epsilon < \epsilon_0 \approx 0.01$), while dramatically increasing after ϵ_0 .

Further study shows that in the DSC region a dramatic increase of the order parameter comes from a symmetry breaking of the state; this symmetry breaking establishes certain phase organization and spatial ordering between various oscillators and produces the oscillation of $S_{ij}(\tau)$ with large amplitude. At $\epsilon = 0$, the system has an orientation symmetry, i.e., the state is invariant, regarding the alternation of the clockwise and anticlockwise directions; this orientation symmetry keeps until $\epsilon < \epsilon_0$ in a disordered region, while it breaks as the order parameter grows after $\epsilon > \epsilon_0$.

In order to show this symmetry breaking, we compute the phase angles of all oscillators in the x - y plane $\tan\phi_i = y_i/x_i$, $i = 1, 2, \dots, 6$. In Figs. 3(a)–3(c), we plot the instant phase distributions for $\epsilon = 0.005$ (DSC region), 0.016 (DSC region), and 0.100 (PSC region), respectively, by rescaling the amplitudes of all oscillators to unit. It is found that in 3(a) the angle distribution is random (called random-phase state), in 3(b) the distribution is such that the oscillators are organized in an anticlockwise direction and the angle between each pair of neighbor cells become phase locked to each other and fluctuate around $\frac{2\pi}{6}$, and in 3(c) each oscillator has approximately the same phase. An extremely interesting point is that a spontaneous orientation symmetry breaking occurs from 3(a) to 3(b). This coherent phase relation between different oscillators after the symmetry breaking leads to the large deviation of $S_{ij \neq i}(\tau)$ from $\sqrt{2}$ in Fig. 2(b), and then is responsible for the fast increase of the value of the order parameter ΔS in Fig. 2(g) after $\epsilon > \epsilon_0$.

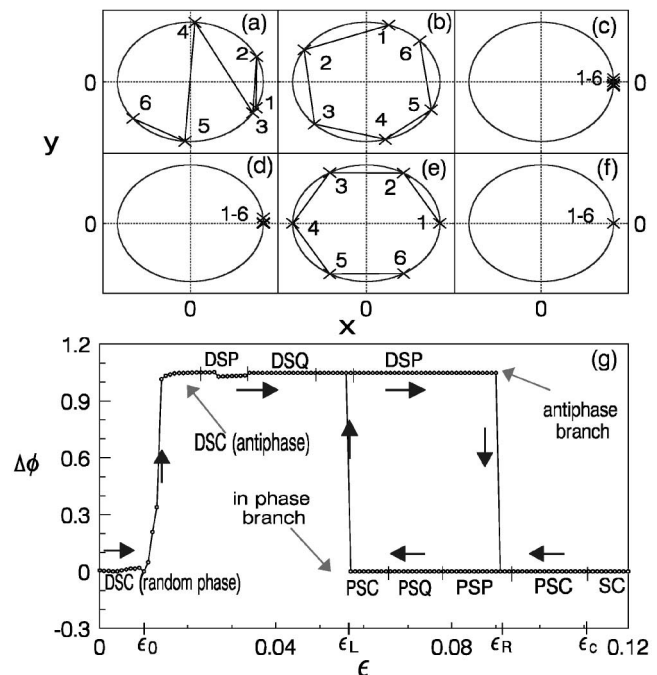


FIG. 3. (a), (b), (c) Instant distributions of phases of all oscillators. (a) $\epsilon = 0.005$ (random-phase DSC state). (b) $\epsilon = 0.014$ (ordered phase DSC state). (c) $\epsilon = 0.100$ (PSC state). (d), (e), (f) Average distributions of phases of all oscillators for the parameters, corresponding to (a), (b), and (c), respectively. (g) The absolute phase difference $\Delta\phi = |\phi_{12}|$ vs ϵ . In the interval $\epsilon \in (0, \epsilon_0)$, we have approximately $\Delta\phi = 0$, indicating random-phase distribution. We observe an antiphase state with $\Delta\phi = \frac{2\pi}{6}$ for the Fig. 1(d) branch, and an in-phase state with $\Delta\phi = 0$ for the Fig. 1(c) branch. First-order phase transitions between the two branches occur at the turning points ϵ_R and ϵ_L .

From previous papers, we are familiar with the terminologies of “in phase” and “antiphase,” which were used in describing the phase relations between periodic oscillators for exactly equal phases and equal phase differences [5], respectively. Thus far, the antiphase state has never been found in chaotic systems. Here, by means of a long time average, we can identify the in-phase and antiphase states for chaotic coupled oscillators. In Figs. 3(d)–3(f), we plot the average angles, corresponding to the parameters of 3(a)–3(c), respectively, by setting $\phi_1 = 0$ and computing

$$\Delta\phi_{ii+1} = \frac{1}{n} \lim_{n \rightarrow \infty} \sum_{\mu=1}^n \Delta\phi_{ii+1}(\mu), \quad (4)$$

$$\Delta\phi_{ii+1}(\mu) = \phi_{i+1}(\mu) - \phi_i(\mu),$$

where $\phi_i(\mu)$ is the angle value of the i th oscillator at time $\mu\Delta t$, $\Delta t = 0.5$. $\Delta\phi_{ii+1}(\mu)$ takes value in $(-\pi, \pi)$. Exact antiphase and in-phase statuses are obviously shown in 3(e) and 3(f). In Fig. 3(g), we plot $\Delta\phi = |\Delta\phi_{12}|$ vs ϵ , and find, reasonably, $\Delta\phi = 0$ in the random-phase region (i.e., the spatially disordered chaos region of $\epsilon < \epsilon_0$). After $\epsilon > \epsilon_0$, $\Delta\phi$ jumps to $\frac{2\pi}{6} \approx 1$, and the system establishes spatial order of antiphase relation between various oscillators. *This antiphase distribution keeps in the entire branch of Fig. 1(d) for $\epsilon > \epsilon_0$ independent of the system being chaotic, periodic, or quasiperiodic.* The sharp jump of $\Delta\phi$ at ϵ_0 indicates a clear phase transition, explaining the behavior of Figs. 2(b) and 2(g). Unlike the first order bifurcations at ϵ_L and ϵ_R , the phase transition at ϵ_0 is of second order with a single symmetry breaking. In the branch of Fig. 1(c), we have an *identically in-phase relation of $\Delta\phi = 0$ between all oscillators in all SC, PSC, PSP, and PSQ regions.* Though in both random-phase and inphase regions we have $\Delta\phi = 0$, the two situations are totally different [see Figs. 3(a) and 3(c)].

In summary, we have investigated the evolution from high-dimensional spatiotemporal chaos to low-dimensional synchronous chaos by increasing ϵ from zero to $\epsilon > \epsilon_c$. For $\epsilon > \epsilon_c$ the system is chaotic in time and synchronized and completely symmetric in space. For $\epsilon = 0$ the system is chaotic in time and random while macroscopically symmetric in space. In the middle range of ϵ we find rich bifurcations (both first order and second order) leading to various states which may be chaotic, quasiperiodic, and periodic in time, and partially synchronized or desynchronized in space. Different types of symmetry breakings link all these variations. The most important findings of this paper are the following. (i) Decreasing ϵ lower than ϵ_c , the synchronous chaos desynchronizes to a chaotic state with partial synchronization, associated with a breaking of spatial translation symmetry. This PSC state can bifurcate to periodic and quasiperiodic states with the same typical

spatial structure. (ii) Increasing ϵ higher than ϵ_0 , the disordered desynchronized chaos bifurcates to an ordered desynchronized chaos (a novel phase transition) with equal (in the sense of average) phase shift between neighbor oscillators (a novel antiphase chaos), associated with an orientation symmetry breaking in space. This antiphase chaos can bifurcate to various periodic and quasiperiodic states with the same spatial antiphase structure. (iii) The results of Fig. 3(g) are also significant. We find an in-phase branch starting from the synchronous chaos and antiphase branch bifurcated from the chaos with random phase distribution. By increasing ϵ from zero to $\epsilon > \epsilon_c$ we can find that synchronization increases step by step: from random-phase desynchronous chaotic state to coherent antiphase desynchronous states, to partially synchronous in-phase states, and, finally, to a completely synchronous state. This general picture links well the rich and complicated patterns of coupled systems. (iv) The in-phase branch keeps orientational symmetry while breaks translational symmetry, and the antiphase branch is just the opposite. Since, in general, no continuous bifurcation can exchange these two symmetries simultaneously at a same bifurcation point, the first-order transitions and the hysteresis loop between the in-phase and antiphase branches in Fig. 3(g) can then be anticipated. We have confirmed its generality for coupled Rossler oscillators for different N , like $N = 5, 7, 14, 15, 50$, and we are planning to generalize this kind of study to other coupled systems.

This work was partially supported by the National Natural Science Foundation of China and the Nonlinear Science project of China.

-
- [1] J.F. Heagy, T.L. Carroll, and L.M. Pecora, Phys. Rev. E **50**, 1874 (1994); A. S. Pikovsky, M. G. Rosenblum, G. Osipov, and J. Kurths, Physica (Amsterdam) **104D**, 219 (1997); A. S. Pikovsky, G. Osipov, M. G. Rosenblum, M. Zaks, and J. Kurths, Phys. Rev. Lett. **79**, 47 (1997); L. M. Pecora and T. L. Carroll, Phys. Rev. Lett. **80**, 2109 (1998); G. Hu, J. Z. Yang, W. Q. Ma, and J. H. Xiao, Phys. Rev. Lett. **81**, 5314 (1998); E. Rosa, Jr., E. Ott, and M. Hess, Phys. Rev. Lett. **80**, 1642 (1998).
 - [2] C. M. Gray, P. Koenig, A. K. Engel, and W. Singer, Nature (London) **338**, 334 (1989); K. Kaneko, in *Statistical Physics (STATPHYS 19), Proceedings of the 19th IUPAP International Conference on Statistical Physics, Xiamen, China*, edited by Bai-Lin Hao (World Scientific, Singapore, 1996), p. 338; K. Otsuka, *Nonlinear Dynamics in Optical Complex Systems* (Kluwer, Dordrecht, 2000).
 - [3] M. G. Rosenblum, A. S. Pikovsky, and J. Kurths, Phys. Rev. Lett. **76**, 1804 (1996); **78**, 4193 (1997).
 - [4] C. van Vreeswijk, Phys. Rev. E **54**, 5522 (1996); M. Hasler, Y. Maistrenko, and O. Popovych, Phys. Rev. E **58**, 6843 (1998).
 - [5] K. Wiesenfeld, C. Bracikowski, G. James, and R. Roy, Phys. Rev. Lett. **65**, 1749 (1990); S. Nichols and Kurt Wiesenfeld, Phys. Rev. E **50**, 205 (1994).